Fan Acoustic Flight Effects on the PAA & ASN Flight Test

Ian A. Clark*, Russell H. Thomas†, and Yueping Guo†
NASA Langley Research Center, Hampton, VA 23681 USA

Accurate and reliable prediction of noise emitted from turbofan aircraft engines is an ongoing challenge. For continued progress, it is necessary to assess the performance of the most recent prediction methods in the NASA Aircraft NOise Prediction Program (ANOPP), and to examine the effects of flight condition on fan noise. The assessment is based on an extensive acoustic dataset acquired as part of the Propulsion Airframe Aeroacoustics and Aircraft System Noise (PAA&ASN) Flight Test conducted as part of the Boeing 2020 ecoDemonstrator program on a 787-10 Etihad Airways airplane. Engine operating condition was varied to study the characteristics of fan noise in flight. In a subset of the flight test matrix, the influence of the aft duct acoustic liner was studied by covering the lined area with aluminum tape to simulate a hardwall duct. The combination of test data at different flight conditions, along with rigorous predictions of jet noise, is used in this paper to extract fan noise from the measured total aircraft noise levels. The measured fan noise levels are compared with those predicted using the latest methods for fan source noise, liner attenuation, and PAA effect prediction. Detailed analyses are undertaken to understand agreement between data and various aspects of the prediction models, including spectral shape, directivity, and response to throttle setting. An additional investigation was undertaken to study the effect of aircraft speed on fan noise, as current models do not directly account for this parameter.

I. Introduction

The overarching goal of the NASA Advanced Air Transport Technology (AATT) Project is to explore and develop technologies and concepts for improved energy efficiency and environmental compatibility for fixed-wing subsonic transports. The knowledge gained from AATT research – in the form of experiments, computations, data, system studies, and analyses – is critical for conceiving and designing cleaner, quieter, and more efficient aircraft. The AATT Project will identify and mitigate technical risk as well as transfer knowledge to the aeronautics community at large so that new technologies and vehicle concepts can be incorporated into the future design of aircraft [1].

The AATT Project is continually improving the quality of system noise assessments of current and prospective aircraft. Full-scale flight data are a critical means of improving and validating system noise assessment tools, including the NASA Aircraft NOise Prediction Program (ANOPP). In addition to validation of existing models, data from carefully designed full-scale flight experiments allow for the opportunity to develop additional models, add capability to existing models, and enhance the understanding of the effects from integrating the propulsion system with the airframe. These Propulsion Airframe Aeroacoustics (PAA) integration effects have been shown in previous research [2, 3] to be the largest differentiators between future advanced aircraft concepts. In a recent study [3], a Hybrid Wing Body (HWB) aircraft was calculated to be 16.1 EPNdB cumulative quieter than an equivalent engine-under-wing aircraft, with 10.7 EPNdB of that difference resulting directly from PAA effects.

Fan source noise, the performance of engine acoustic liners, and PAA effects associated with fan noise are key elements of system noise, even for aircraft concepts that feature significant engine noise shielding. June et al. [4] found that a strong majority of uncertainty present in the system noise prediction of an HWB aircraft could be attributed to the prediction of fan source levels, engine acoustic liner performance, fan PAA effects, and Krueger flap noise. Multiple studies [5–7] have found that even for an engine-over-wing configuration with shielding, reduction of fan noise would still significantly reduce community noise, especially for observers not directly beneath the flight track. Beyond this, recent studies [3, 8–10] of NASA concepts have identified fan noise with liner and PAA effects to be a dominant source when simulating noise at the approach, lateral, and flyover FAA certification measurement locations [11]. NASA has funded research on Truss-Braced Wing configurations both internally and externally [12] since 2010, and the most recent acoustic assessment of the concept [13] shows fan noise, liner, and PAA effects to be critical to the overall noise

and key targets for noise reduction technology. In spite of the demonstrated importance of fan noise, liner effects, and PAA effects, few comprehensive flight research experiments have been performed to rigorously evaluate the modeling of these effects. One recent study of note is the flight test of the NASA Advanced Inlet Liner on the Boeing Quiet Technology Demonstrator 3 [14–16], during which a multidegree-of-freedom (MDOF) liner was tested in the inlet of a Boeing 737 MAX-7 aircraft. However, that test was focused on the performance of the new liner technology specifically and did not study the fan source levels, aft liner performance, or PAA effects in detail.

To address the knowledge gaps identified above, the Propulsion Airframe Aeroacoustics and Aircraft System Noise (ASN) flight test was performed in August 2020 in collaboration with The Boeing Company as part of the ecoDemonstrator 2020 program. The test was carefully designed for high signal-to-noise ratio and repeatability, yielding a complete dataset with which to evaluate many of the models that comprise ANOPP, including those for fan noise and liner effects. Furthermore, the campaign allowed for an in-depth study of the unique PAA effects of a modern airliner through a full-fidelity experiment, during which all full-scale flight effects were included. This dataset is impossible to obtain in a wind tunnel. Multiple objectives were undertaken over five days of flying. An overview of the full experiment is presented in companion papers by Thomas et al. [17] and Czech et al. [18].

The focus of the study presented in this paper is an assessment of the accuracy of the overall fan noise prediction methodology on a state-of-the-art aircraft at full scale, including flight, PAA, and engine liner effects. In particular, comparisons will be made between measured fan noise levels and the fan noise prediction of the internal research version of ANOPP (ANOPP-Research) used in recent studies [2, 3, 8–10]. The most recent fan noise prediction method in ANOPP-Research was developed by Krejsa and Stone [19] utilizing wind tunnel data from the 9- by 15-foot Low-Speed Wind Tunnel at the NASA Glenn Research Center [20]. The method was developed using data from one fan, and the resulting model compared well with the noise measured from a different fan in the same wind tunnel. The model utilizes the same form as the original Heidmann method [21], but is recalibrated for application to fans of modern high bypass ratio turbofan engines. The primary method for predicting acoustic attenuation from conventional liners is the General Electric (GE) method developed by Kontos et al. [22], but liner technology has developed significantly since the model development 25 years ago. Finally, prediction of PAA effects in recent NASA studies has followed a data-driven approach, which will be utilized here and described in further detail in later sections. This paper compares the results from these prediction methods to the full-scale data collected in the flight test.

Section II provides an overview of the test setup. Section III describes the process by which fan noise was extracted from the measured total aircraft noise. Section IV describes the process by which ANOPP-Research was used to produce a complete prediction of fan noise. Section V compares the measured and predicted levels, both in absolute terms and after normalization to focus on spectral shape, directivity, and the response to throttle setting. Section VI summarizes an investigation into the effect of aircraft speed on fan noise. Finally, Section VII presents the study's conclusions.

II. Flight Test Setup

The test was performed in collaboration with The Boeing Company as part of their 2020 ecoDemonstrator program. This test utilized a newly manufactured Boeing 787-10 Etihad Airways airliner. The aircraft's wingspan is approximately 197 feet, and the fuselage length is approximately 224 feet. The General Electric GEnx-1B engines feature a bypass ratio of approximately nine at takeoff. For flight conditions that supported engine noise measurements, the port engine was designated as the test engine and was set at a target N1C (corrected fan shaft rotation speed), while the starboard engine was kept at flight idle. This was done to isolate the noise from a single engine, and to study the unique PAA effects of a single engine. For this test, the aircraft was outfitted with an extensive suite of instrumentation, including flight data recorders for highly accurate, time-resolved aircraft state telemetry during the test, in addition to over 200 Kulite surface pressure transducers placed strategically on the exterior surface of the fuselage and wing. The data collected by the Kulites are not the focus of this paper, but will be discussed in detail in a future publication.

The test was conducted near Glasgow, MT at a privately-owned airfield with no other air traffic in the vicinity. This, along with the remote placement of the airfield, provides an ideal environment for acoustic testing with background noise limited mainly to wildlife. Weather conditions were also favorable for acoustic testing, and those requirements are described in more detail by Czech et al. [18]. Ground-based acoustic instrumentation included a 960-microphone phased array setup on the runway overrun area and eight community microphone arrays with 42 ground-board microphones in total. A portion of the instrumentation systems can be seen in the photograph in Figure 1. The design and implementation of the instrumentation systems used in this test are discussed in detail in Czech et al. [18]. This paper focuses primarily on data captured from the community microphone arrays, which provide a view into the directivity of the total aircraft noise. By focusing analysis on aircraft conditions where certain components are known to be dominant,
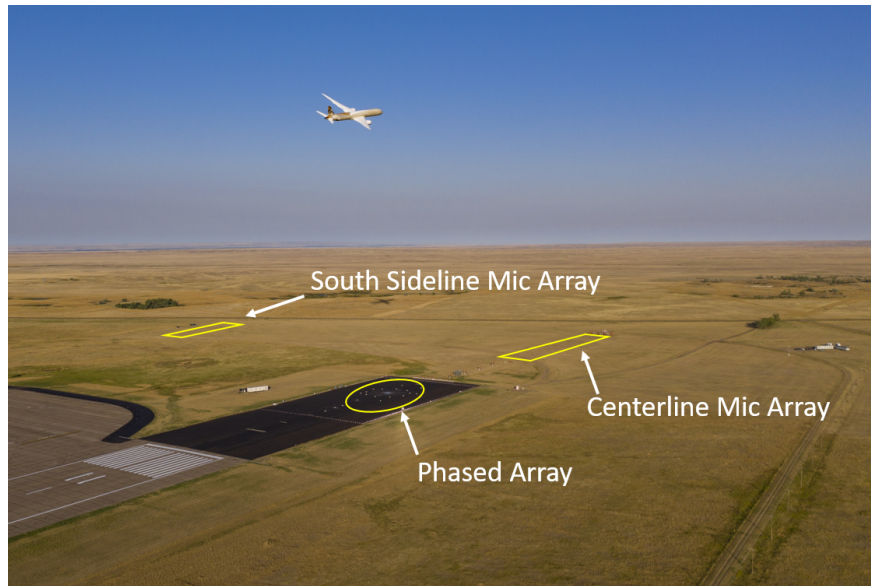
Fig. 1 Drone photograph of test aircraft flying over acoustic instrumentation. Array locations highlighted in yellow for clarity. Not all arrays are shown/highlighted. Photo credit: The Boeing Company.

these microphones can be used to infer directivity of single noise sources as well. The community microphones were laid out in linear arrays running parallel to the runway and flight path, as shown in Figure 2. The centerline array, measuring the direct overhead noise, was deemed the most critical and so was comprised of eight microphones for maximum repeatability and high-quality averaging. The farthest lateral array positions, at 1476 ft off the centerline, were chosen to match the lateral offset of microphones used for the lateral aircraft noise certification point as specified in Title 14 of the Code of Federal Regulations, Part 36 [11], and each contained four microphones for averaging. The intermediate arrays were placed to provide a representative sampling of directivity angles, with each array containing three microphones for averaging. For the sake of brevity, all measured data and predictions shown in this study will be obtained from the centerline microphone array.

For each flyover measurement discussed in this paper, the aircraft traveled along a flight path that followed the runway centerline. The exact three-dimensional flight path to be flown during the test was determined by flight test engineers, who factored in the engine throttle set point, high lift and gear configuration, fuel and payload, etc. in order to meet a set of constraints on aircraft altitude and speed over the microphones. If any critical variable was out of tolerance or varied too much during the flyover, the run was considered unusable and was repeated. Due to the variation in aircraft and engine set points during the test, this resulted in a range of variable flight parameters (airspeed, flight path angle, angle of attack, etc.). After the test, the acoustic data collected by the community microphones were processed to represent data from a normalized flight path. Unless otherwise noted, for the runs considered in this paper, this normalized flight path followed a 4 degree climb, with a 4 degree angle of attack at 180 knots, passing through 800 ft altitude above ground level at the center of the microphone arrays. The process by which the data were normalized to this flight path followed standard procedures also applied for noise certification testing. This normalized flight path removes the confounding effects of aircraft position on the acoustic results and isolates the noise differences due to the variable(s) of interest, such as throttle setting, aft duct liner configuration, or aircraft speed.

A variety of aircraft configurations were measured throughout the five test days. For one test day, the test engine was modified to cover the acoustic liner in the aft fan duct with aluminum tape, mimicking a hardwall duct and removing the acoustic effect of the liner in this area. With this configuration, a series of flyovers at a range of throttle conditions was performed in order to measure the engine noise without the aft acoustic liner attenuation. In addition, several throttle conditions were repeated with varying airspeed to measure the change in noise. After removal of the aluminum tape to restore the engine to its production configuration, the same conditions were repeated on the following day to measure the effects of the liner on the noise at varying throttle conditions and airspeeds. These test conditions are the focus of this paper. Other test conditions were flown to study the acoustics of the airframe (high lift system, landing gear, etc.), as well as other PAA effects, and these conditions will be presented in companion [23] and future publications.
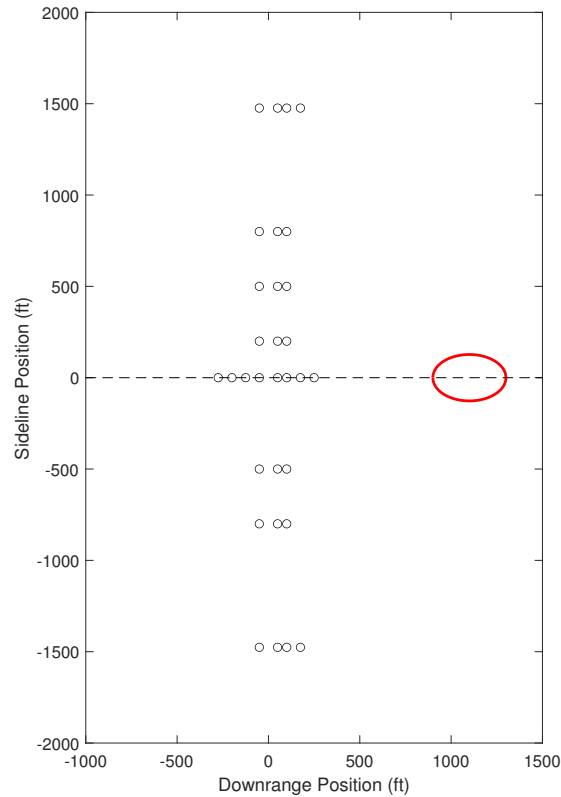
Fig. 2 Community microphone (black circles) and phased array (red oval) locations. For the flights considered in this publication, the flight path was from right to left along the dashed line.

III. Data Processing

Although the acoustic data were normalized to a standard flight path prior to delivery to NASA, the reported levels still required post-processing to make them suitable for the present analysis. The reported one-third octave band sound pressure levels ($SPL_{1/3}$) represented the measured flyover noise of the complete aircraft, with all sources present, including engine and airframe sources. Although the flaps were set to the takeoff detent for all flyovers, airframe noise was a nonnegligible contributor to the overall aircraft noise, particularly at lower engine throttle settings. In addition, fan noise was not the only engine source present, as jet noise was also expected to contribute significantly to the overall levels. Prior to looking deeper into the results, it was necessary to analytically subtract these other sources to isolate the fan noise spectra and minimize contamination from these other sources of noise.

A. Engine Noise Isolation

In addition to the engine measurement conditions flown at nominally 180 knots with takeoff flaps and retracted landing gear, a similar flyover was conducted with two primary differences. First, both engines were set to flight idle to minimize engine noise. Second, because of the low thrust setting, it was necessary to fly a descending flight path toward the runway, in the opposite direction of the other engine measurement flyovers that followed a takeoff flight profile away from the runway. Because the engines were set to a very low power setting to minimize engine noise, this configuration provides the best possible measurement of the airframe noise that would contribute to the overall levels of the other engine measurement conditions. These levels can be subtracted, on a pressure-squared basis, to remove the airframe noise levels from the full aircraft levels, thereby isolating engine noise. Before this could be completed, however, it was necessary to analytically shift the flight path from the as-flown approach flight path to the takeoff flight path, in order to ensure that the spectral subtraction was performed on an equal basis.

One-third octave band spectral levels were provided for a series of aircraft emission angles, defined as the angle between the engine axis and the direct path to the ground observer (microphone). For each emission angle, the aircraft altitude and propagation distance to the microphones were also reported. The altitude at each emission angle was used to calculate an average atmospheric absorption coefficient for an acoustic standard day using the SAE ARP 866A [24] standard method (spectral levels had already been corrected to an acoustic standard day). Then, based on the difference in propagation distances between the takeoff and approach flight paths for each emission angle, the effects of spherical spreading and atmospheric absorption were added/subtracted as appropriate to arrive at levels that would be expected for the takeoff flight profile.

With spectral levels representing airframe noise and total aircraft noise on an equivalent basis, the spectra were subtracted on a pressure-squared basis to yield isolated engine noise. For the subtraction, the total aircraft levels had to be a minimum of 0.5 dB above the airframe levels before the subtraction could be performed. If this criterion was not met at a given frequency, it was assumed that the engine noise could not be reliably separated from the airframe noise, and the data point was removed from the resulting spectrum.

B. Fan Noise Isolation

With engine noise effectively isolated, attention can be turned to isolating fan noise specifically. Engine noise can be expected to be a sum of noise from the fan, jet, combustor, turbine, compressor, and other auxiliary components. As the strengths of these sources are all dependent upon engine throttle setting, it is impossible to choose an engine condition that would isolate any of these sources for subtraction. Therefore, a different method must be used. Following the methodology of Krejsa and Stone [19], semiempirical methods can be used to predict the expected levels of the individual engine components at each engine operating condition. These predicted levels can then be subtracted from the total measured engine levels to isolate the component of interest. No information was provided for the engine core, so core noise could not be predicted. Therefore, for the present study, it is assumed that the only other dominant component of engine noise is the jet.

In order to predict jet noise, the method of Stone et al. [25] is used as implemented within the research-level ANOPP code (ANOPP-Research). The necessary inputs to the method were provided by Boeing through the use of their internal modeling of the GEnx engine on the 787 aircraft. Two key features of jet noise prediction within ANOPP-Research, as compared to the released version of ANOPP, are the angle-of-attack correction to the computed jet noise and the inclusion of PAA effects, specifically noise reflection from the airframe. The aircraft angle of attack was recorded at a 5 Hz sample rate throughout each flyover, and the average value for a given flyover was used to calculate the acoustic correction. To incorporate PAA effects and include the scattering of jet noise from the airframe, a data-driven approach was utilized using measured data from a previous experiment in the Boeing Low-Speed Aeroacoustic Facility (LSAF) [26]. In that experiment, a realistic high-bypass ratio jet nozzle was operated with heated flow to simulate the jet noise at various engine operating conditions. The jet simulator was tested in both an isolated configuration and integrated with a 777 airframe model, and the measured acoustic difference was used as an amplification factor to the jet noise predicted for the present study after the results were appropriately scaled up to full scale. With jet noise computed using the specific inputs applicable to each measurement condition, the noise was analytically propagated from the normalized takeoff flight path to each observer location on the ground to prepare it for subtraction from the measured engine levels. As was done during the airframe noise subtraction, a minimum difference of 0.5 dB was required to obtain spectral levels from the subtraction.

With these calculations completed, the fan noise was effectively isolated in the measured data, allowing for direct comparisons with predicted levels from the method of Krejsa and Stone [19]. However, it is important to keep in mind the assumptions made during this isolation process when analyzing the comparisons. The measured fan noise levels reported later are functions of the airframe and jet noise spectra obtained above, which means a change or update to the airframe data processing or jet prediction will yield a change in measured fan noise after subtraction.

To simplify the comparisons between the measured data and the model and to remove differences due to different propagation effects, the measured levels were back-propagated to a 1-ft source hemisphere, thereby removing the effects of spherical spreading and atmospheric absorption. Predicted levels were computed directly at this 1-ft source hemisphere, again using ANOPP-Research. Although the effects of Doppler frequency shift and convective amplification were not removed, both the measured and predicted levels would be affected equally, so the comparisons to follow are established on an equivalent basis.

5

IV. ANOPP-Research Prediction

To facilitate a comparison between the measured fan noise levels and those predicted by the method of Krejsa and Stone [19], ANOPP-Research is again used since the method is implemented in the code. In general, the fan source noise prediction method can be considered to have three primary functional dependencies for each component. The first is a series of source strength functions that are dependent on mass flow rate, total temperature rise across the fan, relative tip Mach number, and rotor-stator spacing. In flight, the first three of these four parameters are dependent upon throttle setting. Once the source strength has been established, the second functional dependency is a directivity function that describes how the peak level varies with emission angle (fore to aft). Finally, the third functional dependency is a spectral shape function that determines the peak frequency and relative variation with frequency. The method breaks down the overall fan noise prediction into separate components, namely inlet- and aft-radiated broadband and tonal noise. However, due to the nature of the flight test measurements and data processing, these predicted components will be combined into a single fan noise prediction for purposes of comparison with data. For this study, inlet- and aft-radiated broadband and rotor-stator interaction tones were computed and combined to yield a complete prediction of fan noise. Combination tones were excluded from the ANOPP-Research predictions for reasons outlined in Section V. All input values necessary for a prediction were provided for each flyover by Boeing through the use of their engine cycle analysis tools. Relevant geometric parameters necessary for the prediction were also provided for the fan and for the inlet and aft duct liners.

Although the specific liner locations within each duct are known, the General Electric method of computing liner attenuation accepts only simple inputs of lined duct height and length. For the inlet duct, these values are largely representative of the overall liner layout. However, the aft duct liner coverage is more complicated to accommodate different engine components and moving parts within the duct. In order to simulate the aft duct in a repeatable way, the aft duct height (difference of outer and inner diameters) was first set to the average value of the GEnx engine. Since the length parameter in the liner model sets the overall attenuation level, the length was calculated such that a fully-lined annular duct (as modeled in the GE method) would contain the same liner area as was present in the actual engine. A 10% increase in liner length is included to account for advancements to liner technology since the development of the GE method, such as spliceless liners.

It is important to remember that the fan noise prediction method considered here was developed from data collected from an isolated fan test rig in a wind tunnel, with no scattering surface (such as a wing) present. Because the prediction method does not account for this physical difference, the presence of the wing must be accounted for using a separate method. In this study, a data-driven approach is used to model the PAA effect of the reflecting surfaces near the engine. An experimental database of PAA measurements was developed in previous work through extensive wind tunnel tests in the Boeing LSAF [27]. To simulate the compact, broadband characteristics of a fan noise source, a collection of impinging jets was installed within a model-scale nacelle. Measurements were taken in the far-field at a range of directivity angles for both the isolated source within the nacelle, as well as with the source/nacelle placed near a scale model of a 777 airframe. The facility design permitted easy relocation of the airframe relative to the noise source such that a wide array of simulated engine locations could be measured. In addition, the model 777 airframe featured reconfigurable leading and trailing edge high lift devices, and the wind tunnel free-stream velocity was varied. The database therefore contains measured PAA effects that are applicable to a wide range of aircraft operating conditions. By taking the difference between data collected with and without the airframe present, the appropriate amplification factor is determined as a function of directivity and frequency. After converting to full-scale frequencies using the GEnx dimensions, this factor can be applied to predicted fan noise to simulate PAA effects.

An appropriate dataset that most closely matches the 787 operating condition under consideration in this study was selected from the overall database. Since only the port engine was set above flight idle for the cases considered here, care was taken to ensure that the directivity of the PAA model was representative of a single engine on the port side.

V. Results

The results presented here will focus on comparisons between measured fan noise data and predicted fan noise, specifically fan broadband noise and rotor-stator interaction tones. The choice to exclude combination tones that are generated when the blade tip speeds are supersonic, also known as Multiple Pure Tones (MPTs), from the fan noise prediction was made for several reasons. First, preliminary analysis of the narrowband data revealed an absence of significant tonal content below the blade passage frequency, even at the highest engine throttle settings. Second, ANOPP-Research predictions including combination tones were compared with measured data, and it was revealed that the predictions strongly overpredicted the overall system noise at frequencies below the BPF. Excluding the combination

tones from the prediction produced much better agreement across the full frequency range. An example system-level comparison between predicted and measured system-level noise is shown in Figure 3, and additional comparisons and discussion are presented by Thomas et al. [17]. In Figure 3, positive values represent an overprediction relative to measured levels, and it is clear that the inclusion of combination tones causes strong overprediction at forward and overhead angles. Third, after following the component extraction method described in Section III to isolate fan noise, it was found that the majority of fan noise appears at frequencies near and above the blade passage frequency in the measured data, with airframe and jet noise accounting for the majority of system noise below the BPF. Therefore, in order to provide the most representative comparison between ANOPP-Research predictions and measured data, it was decided to exclude combination tones from the prediction and analysis of comparisons to focus primarily on the broadband and rotor-stator interaction tonal components of fan noise. Of course, since the objective of this paper is an evaluation of the current fan noise prediction methods against measured data, this directly leads to the first conclusion of this study, which is that the current process for prediction of combination tones is in need of improvement. The process includes two components: the fan combination tone source prediction and the liner attenuation prediction. As the data used in the development of the fan noise prediction model comes from a hardwall (unlined) test rig, it is difficult to ascertain in which step the majority of the error lies. It is important to note that combination tone noise is known to vary significantly between individual fans, even those of the same design, due to small differences in blade stagger angle or leading-edge contour [28]. The liner attenuation calculation treats all fan noise equally, although it is known that the source generation and propagation of combination tones resulting from supersonic blade tip speeds are fundamentally different than those of other acoustic sources around the fan. Future work will examine this issue in more detail, but the broadband noise and rotor-stator interaction tones will be the focus of the present analysis.

To gain insight into the quality of the fan source noise, liner, and PAA predictions undertaken for this test, four separate comparisons with data will be performed. First, basic comparisons between the predicted and measured noise will be presented and discussed. Next, the predicted and measured values will be processed to focus on each of the three fan noise model components outlined in Section IV, namely spectral shape, directivity, and the response of the source strength to operating condition (referred to here as throttle setting). This enables identification of specific strong and weak points within the fan noise prediction model.

Figure 4 shows relative comparisons between ANOPP-Research fan noise predictions and the measured fan noise data as obtained through the process described in Section III. The flight test matrix of conditions eliminated the lowest thrust point from the production engine campaign, which is the reason for the missing curve in the production cases in Figure 4. It is also noted that the missing spectral values are the result of the minimum difference criterion imposed on the spectral subtraction of both airframe and jet noise as described in Section III. For perfect agreement between predicted and measured levels, all curves would lie directly on the 0 dB axis for all frequencies. Negative values indicate underprediction relative to measured levels. Focusing first on the hardwall aft duct configuration, generally

(a) Combination Tones Included in Prediction

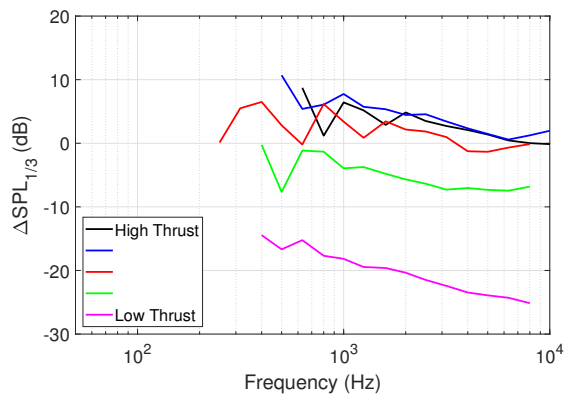(b) Combination Tones Excluded from Prediction
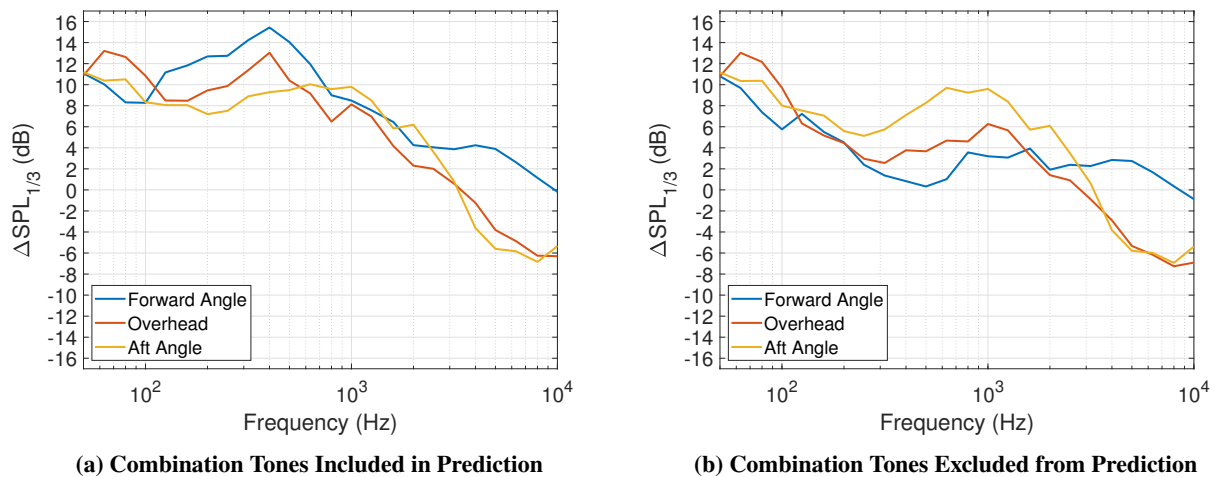
Fig. 3   Differences in aircraft system-level third-octave band SPL predicted using ANOPP-Research and measured levels for the engine at high thrust with production aft duct configuration [17].
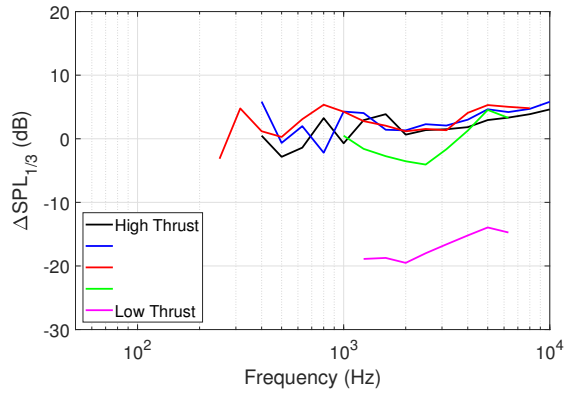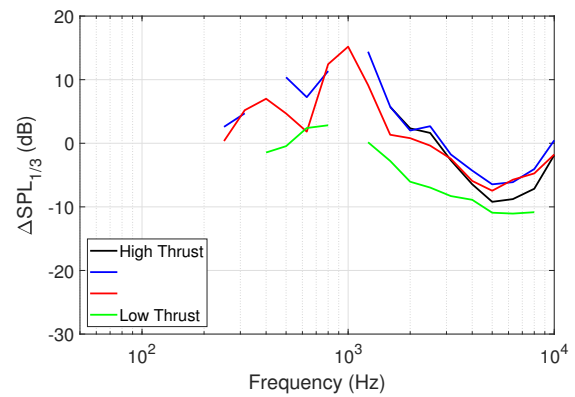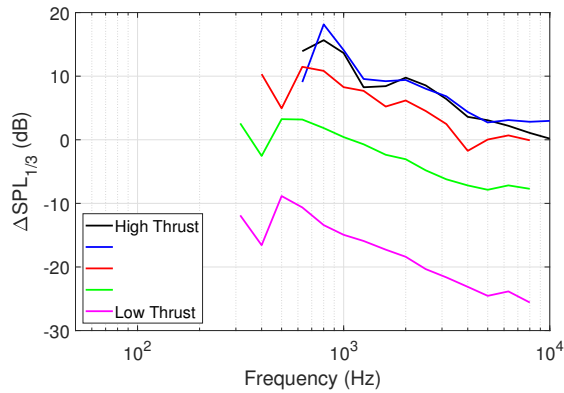
(a) Hardwall Aft Duct, Forward Emission Angle
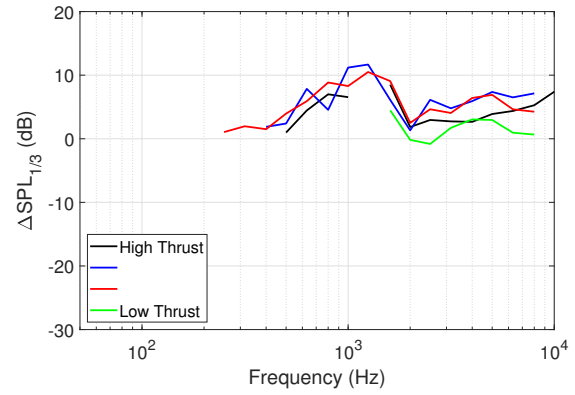
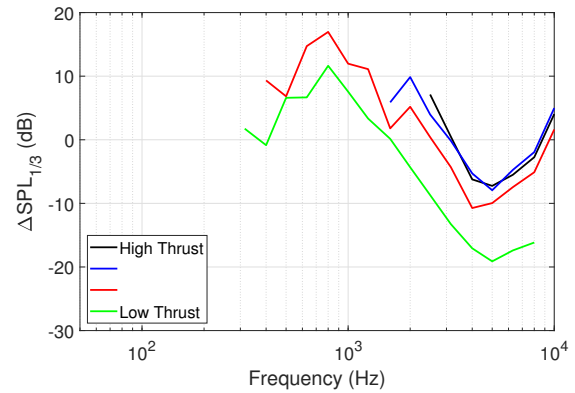**(b) Production Aft Duct, Forward Emission Angle**

(c) Hardwall Aft Duct, Overhead Emission Angle

(d) Production Aft Duct, Overhead Emission Angle

(e) Hardwall Aft Duct, Aft Emission Angle

(f) Production Aft Duct, Aft Emission Angle

Fig. 4   Difference between predicted and measured fan noise levels.

good agreement is observed at the forward emission angle, with the notable exception of the lowest thrust condition, which is significantly underpredicted. At the overhead emission angle, in general, higher thrust values are slightly overpredicted, while lower thrust values are underpredicted. This trend is further exaggerated at the aft emission angle where, at mid- to high-thrust levels, fan noise is strongly overpredicted at all frequencies, up to or above 10 dB over a wide frequency range. At the aft emission angle, a clear dependence on frequency is observed, which can be explained by a shift in the peak frequency between prediction and data causing more overprediction at lower frequencies.

Considering the same comparison for the production aft duct, additional overprediction is observed at the forward angle, an interesting observation considering the inlet duct was unmodified throughout the test. It is thought that some

fan noise radiated from the aft-duct propagated to this forward angle, therefore influencing both the predicted and measured total fan noise spectrum. The overhead angle displays a stronger frequency dependence than was observed for the hardwall duct, suggesting that the liner alters the spectral shape over a different frequency range than is predicted by ANOPP-Research. Again, this trend is exaggerated for the aft emission angle.
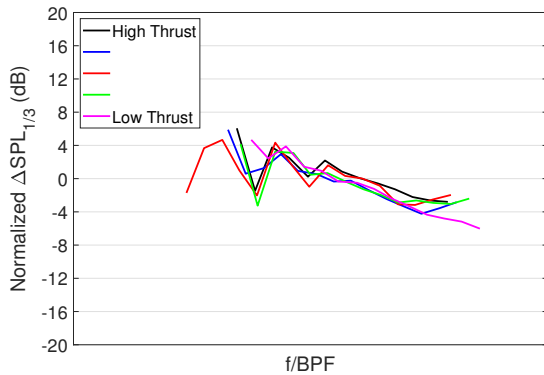
A. Spectral Shape

Figures 5 shows a similar comparison as in Figure 4, with two key differences. First, frequency is normalized to the
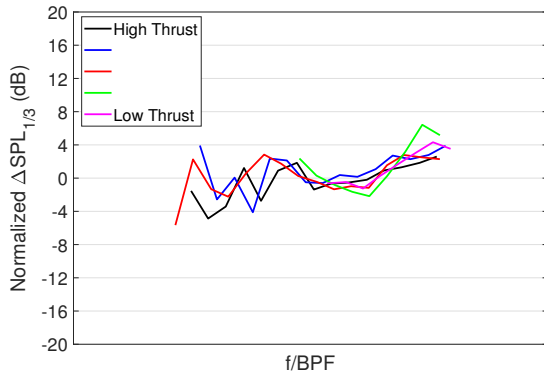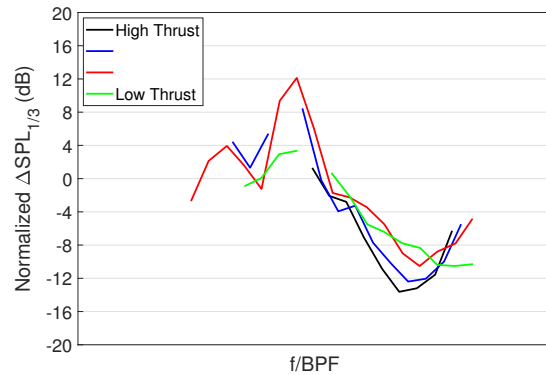

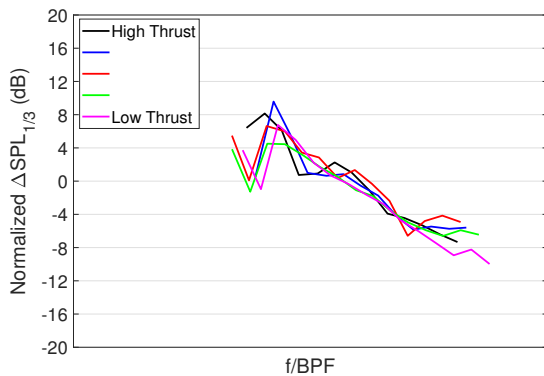(a) **Hardwall Aft Duct, Forward Emission Angle**
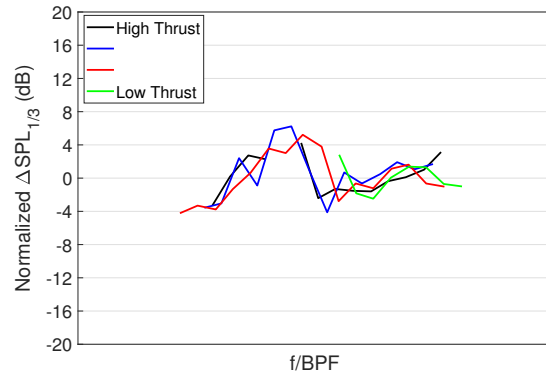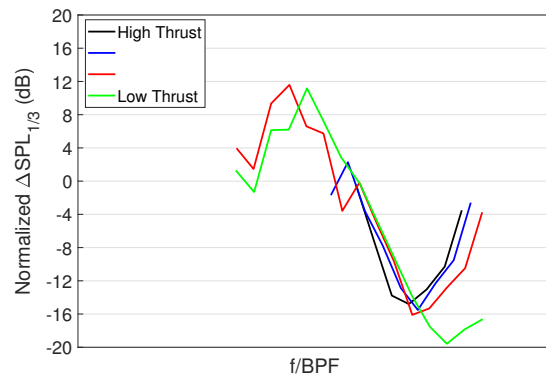
(b) **Production Aft Duct, Forward Emission Angle**

(c) **Hardwall Aft Duct, Overhead Emission Angle**

(d) **Production Aft Duct, Overhead Emission Angle**

(e) **Hardwall Aft Duct, Aft Emission Angle**

(f) **Production Aft Duct, Aft Emission Angle**

Fig. 5 **Normalized difference showing comparison between predicted and measured fan noise spectral shape.**

blade passage frequency (BPF) at each condition considered, thereby eliminating the influence of fan speed and the resulting frequency shift between conditions. Second, the absolute levels of the individual spectra have been normalized on the average of their own highest three $SPL_{1/3}$ values prior to the subtraction between predicted and measured levels. This results in a comparison that is solely focused on spectral shape. For a perfect prediction of spectral shape, the curves would follow the 0 dB line for all frequencies.

Once these normalizations are completed, the resulting plots show a reasonable collapse of the curves for both hardwall and production configurations, although the hardwall configuration does display a tighter collapse than the production configuration. While the spectral trends remain the same as those discussed previously, the collapse of the curves confirms that there is, in fact, a single function that could describe the spectral shape of the measured data with reasonable accuracy, and that this spectral function is independent of engine operating condition. The strong frequency dependence displayed for the aft angle, production aft duct, clearly indicates that there is a mismatch between the predicted and actual target frequencies of the aft duct liner, suggesting that the actual liner attenuation spectrum peaks at a lower frequency than is predicted by the GE method within ANOPP-Research.

B. Directivity

To isolate the directivity effect, the average of the highest three SPLs in each spectrum was used to represent the peak spectral level, denoted here as SPL_{max}. This averaging was performed for each spectrum at each polar directivity angle. Next, for each operating condition, the average peak at each polar angle was normalized relative to the average peak at 90 degrees (overhead) polar angle. Finally, the difference between the predicted and measured normalized average peaks was taken at each angle. These differences are plotted in Figure 6. For a perfect prediction of directivity, the curves would lie on the 0 dB line for all values of polar angle. Positive values indicate that ANOPP-Research predicts more noise than was measured relative to the 90 degree reference angle.

In general, both the hardwall and production aft duct results show similar trends. The plots show good collapse of the curves between approximately 80 and 120 degrees polar angle. This indicates that the directivity in this region is largely independent of throttle setting, and a function could be found to predict the directivity with reasonable accuracy. Aft of 120 degrees, the curves diverge, indicating that either the directivity here is strongly dependent on thrust setting, or that 90 degrees is not an appropriate reference point for the directivity. Since aft-duct radiated fan noise is expected to be dominant at all aft angles, this second option is less likely to be the cause of the divergence, suggesting that a directivity function should account for thrust setting in this region. At forward angles less than 80 degrees, the curves again diverge. However, this behavior is less surprising given that inlet radiated fan noise is dominant in this region, and so it would be expected that 90 degrees might be a poor reference point from which to normalize the directivity results. This illustrates a shortcoming of the present analysis, namely that the inlet- and aft-radiated fan noise components were not separated, as was done by Krejsa and Stone. Future work will seek to use additional measurements from the other instrumentation systems featured on this flight test to improve the source separation and estimate the relative contributions of inlet- and aft-radiated fan noise.
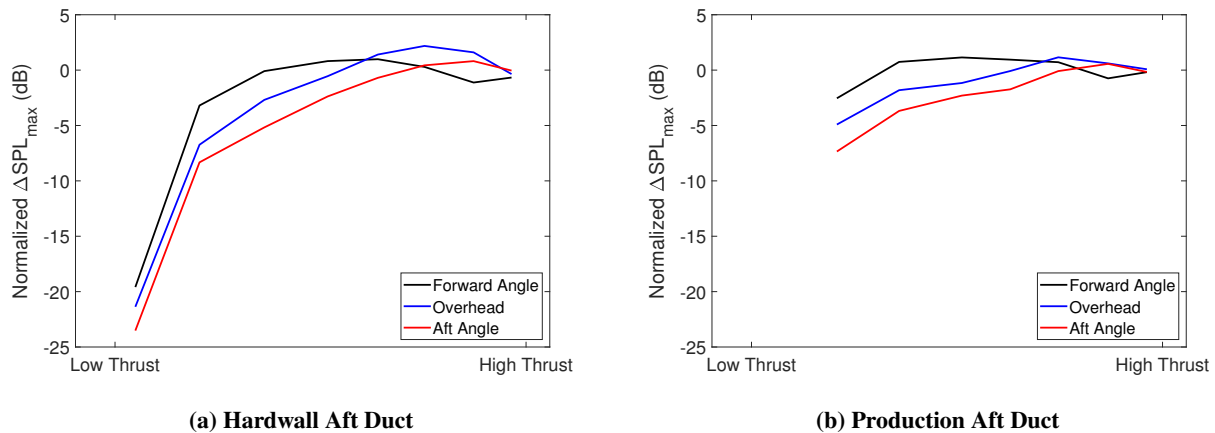

(a) Hardwall Aft Duct

(b) Production Aft Duct
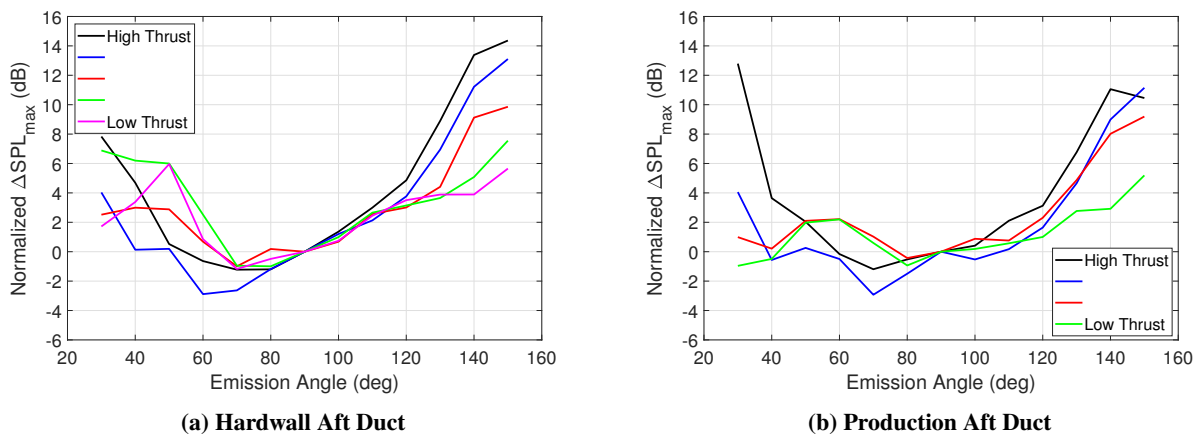
Fig. 6   Normalized difference showing comparison between predicted and measured fan noise directivity.

C. Response to Throttle Setting

To isolate the effect of throttle setting, the average of the three highest SPLs in each predicted spectrum is taken to represent the peak level. Next, the predicted averages for each throttle setting are normalized to the predicted average at the highest throttle setting. This process is repeated separately for the measured averages. Finally, the normalized measured averages are subtracted from the normalized predicted averages at each throttle setting to obtain the plots shown in Figure 7. As such, the delta-SPL values shown in Figure 7 do not represent an absolute comparison between measured and predicted levels, but rather demonstrate the difference between the predicted and measured lapse rate of noise levels as thrust is reduced. For a perfect prediction, the curves would lie on the 0 dB axis for all thrust levels.

First, it is clear that the results show the same overall trends for both the hardwall and production aft duct. The lowest thrust case was not flown with the production aft duct, and so does not appear here. In general, the best agreement appears at the forward emission angle, where inlet-radiated fan noise is dominant, suggesting that the model works reasonably well for inlet-radiated noise, except at the lowest thrust settings. The overhead angle displays a small region of positive values near high thrust levels, indicating that the measured noise decreases faster with small decreases in thrust than ANOPP-Research would predict. However, this quickly transitions to underprediction even at moderate thrust levels. Finally, at the aft emission angle, there is a strong systemic difference in the predicted and actual lapse rates at nearly all thrust levels. ANOPP-Research predicts a much stronger decrease with thrust compared to what is measured. These results indicate that the model for fan noise, particularly the noise radiated from the aft duct, is overly sensitive to engine operating parameters (i.e., mass flow rate, total temperature rise across the fan, and relative tip Mach number).

(a) Hardwall Aft Duct   (b) Production Aft Duct

Fig. 7 Normalized difference showing comparison between predicted and measured fan noise lapse rate with thrust setting.

VI. Flight Speed Effect on Fan Noise

As mentioned in Section II, some flyovers were conducted at higher than the nominal 180 knots flight speed of the previously considered test points. For the production aft duct configuration, two engine operating conditions, representing takeoff and typical cutback power settings, were selected to investigate the effect of flight speed on fan noise by increasing speed to nominally 225 knots. The high lift setting was unchanged from the lower speed flyovers, and the landing gear remained retracted. Engine condition was matched to the lower speed flyovers by matching the corrected fan shaft rotational speed (N1C).

The higher speed flyovers presented additional challenges in isolating fan noise from the measured total aircraft noise. The process described in Section III utilized a flyover at 180 knots with engines idle to subtract the airframe noise from the total noise. This condition is no longer representative of the airframe noise at higher speeds, and no flyover was performed at 225 knots with engines idle. As such, additional processing must be done to the airframe noise data to ensure it is representative of a high speed flyover. In addition, once fan noise is isolated from the high speed powered flyover, propagation effects such as convective amplification and Doppler shift must be accounted for before comparison with the fan noise data from the low speed flyover. This ensures that the comparison is made between levels at the source on an equivalent basis.

Figure 8 summarizes and illustrates the steps involved in this process for both the low and high speed flyovers to enable a one-to-one comparison between the fan noise at the source. Despite the care taken to account for all effects and ensure a direct, equivalent basis for spectral subtraction, the higher airframe noise levels present in the high speed case combined with uncertainties introduced in the processing steps led to a limited frequency range over which fan noise levels could be reliably extracted. The reduced fan source levels at cutback thrust only compounded this difficulty. As a result, Figure 9 displays only a limited dataset from which to make observations. The figure shows the measured differences between high and low speed fan noise levels. Although the results are limited, the reader is reminded that each condition (engine set point, flight speed, etc.) was flown twice to evaluate repeatability. Although not shown here, the absolute levels extracted from the high speed runs were consistent between the two repeated points, which improves confidence in those results. The results from the two repeated runs were averaged to obtain the plotted values. Nonetheless, the discussion here is limited to a qualitative assessment pending further investigation. It is expected that the other instrumentation systems present in the test may be utilized to provide additional information and further insight into the effect of flight speed.

Considering first the takeoff thrust case, the most prominent effect is at the forward emission angle, which shows a clear decrease in levels at high speed compared with the low speed case. The overhead angle is largely unchanged except perhaps for lower frequencies. The aft emission angle results suggest a slight noise increase, a trend that is shared by the cutback thrust case. No forward emission angle fan noise levels could be extracted at cutback thrust. Finally, the overhead levels at cutback thrust show a clear decrease at higher speeds, which is a departure from the results at takeoff thrust. This suggests that the effect of flight speed may be dependent on the engine operating condition, at least at certain emission angles.

While not shown here, it is noted that ANOPP-Research fan noise predictions of the low and high speed flyovers showed no difference in levels, aside from the effects of Doppler frequency shift and convective amplification (the levels matched exactly at the overhead emission angle). Input parameters to the method of Krejsa and Stone, such as mass flow
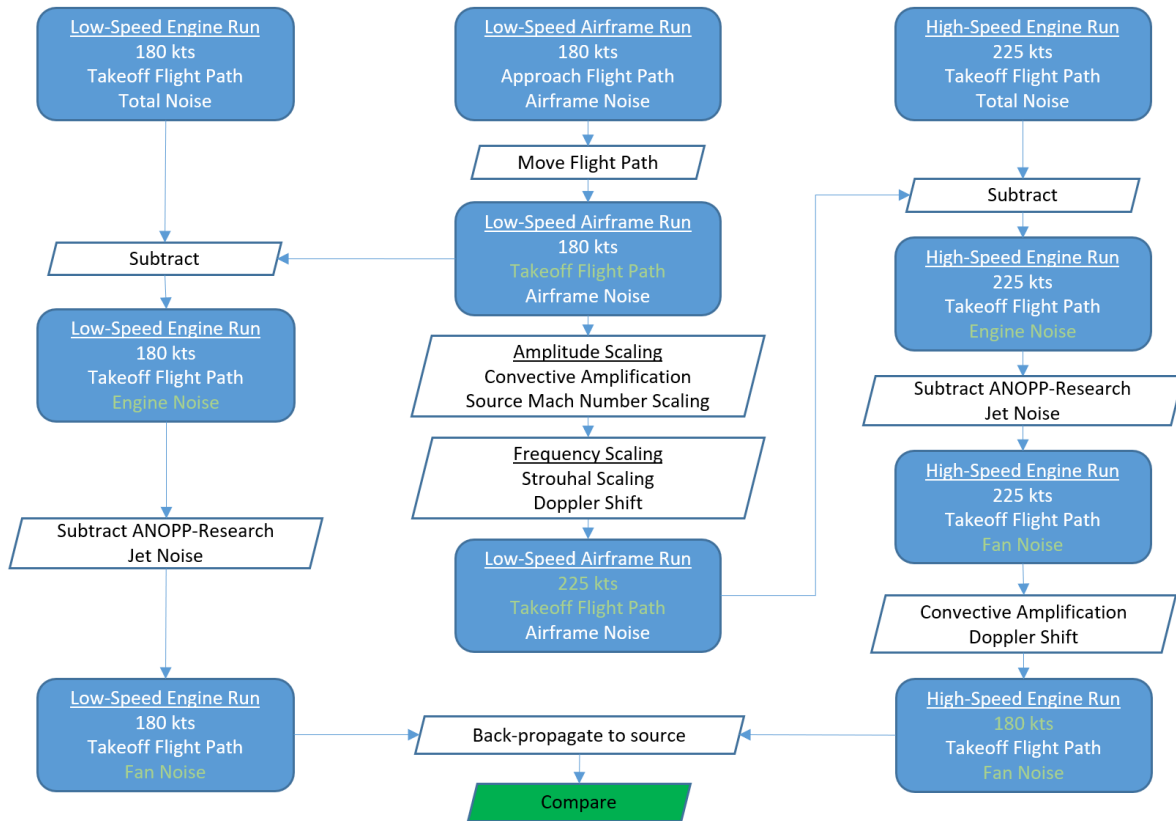
Fig. 8 Process map illustrating the steps required to facilitate comparison between fan noise at low and high flight speed. Green text indicates an analytically altered parameter.

12
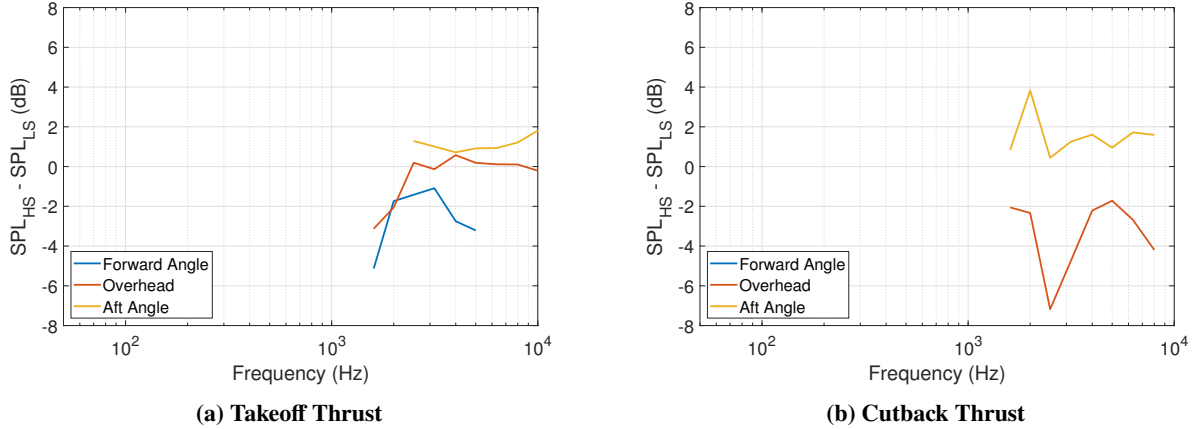
Fig. 9 Measured difference between fan source noise levels at high speed (HS, 225 knots) and low speed (LS, 180 knots) flyovers.

rate, total temperature rise across the fan, etc., were independently calculated using Boeing's engine cycle analysis tools for both the low and high speed cases. Thus, it is clear that the differences shown in Figure 9 are not due to parameter variations that would be captured in the current models.

VII. Conclusions

A comprehensive flight research campaign has been undertaken to complete multiple objectives. As detailed in this study, one of those objectives was a rigorous assessment of fan source noise, acoustic liner performance, and PAA effect prediction methods in ANOPP-Research compared to noise data obtained from a state-of-the-art aircraft in-flight at a range of operating conditions. Through careful processing of the measured data, spectral levels representing fan noise were extracted from the total aircraft noise. Comparisons were made between measured and predicted levels to observe not only overall agreement, but also to establish the relative performance of each aspect of the fan noise prediction.

When setting up the ANOPP-Research predictions, it was determined that the inclusion of combination tones in the fan noise prediction led to significant overprediction of system-level noise. This demonstrates a clear deficiency in the prediction process, which includes both fan source noise and liner attenuation prediction. In order to continue the analysis with an equivalent comparison between predicted levels and observed fan noise characteristics in the measured data, the fan noise prediction included only broadband and rotor-stator interaction tonal noise components. In all comparisons other than directivity, it was observed that agreement between measured and predicted levels was much better at forward angles than for overhead or aft angles, suggesting that the model for inlet-radiated fan noise is more accurate than that for aft-radiated fan noise. Comparisons between predicted and measured levels showed strong overprediction of aft fan noise at aft angles and high throttle settings. Spectral results showed that the peak frequency of aft fan noise was predicted to be lower than the true peak frequency, especially with the aft duct in its production (lined) configuration. This leads to the conclusion that the liner prediction method within ANOPP-Research targeted attenuation at a higher frequency than the actual liner present on the GEnx engine. The directivity results strongly suggest that while aft fan noise directivity is relatively constant with throttle setting near overhead angles, the noise characteristics change significantly with thrust at higher polar angles. Finally, ANOPP-Research predicts a much stronger noise dependence on throttle setting than what is measured, leading to strongly underpredicted fan noise levels at low throttle settings.

A related investigation focused on the effect of flight speed on measured fan source noise levels. Although only a limited frequency range of fan noise levels could be extracted from total aircraft noise for the high speed flyover, the preliminary data suggests that flight speed does play a role in fan noise. At takeoff thrust, a decrease in levels was observed at forward emission angles, while a slight increase was noted at aft emission angles. Similarly, at a representative cutback throttle setting, levels measured at the overhead emission angles were seen to significantly decrease while aft levels again slightly increased. As the current methods within ANOPP-Research do not feature any parameter dependencies related to flight speed other than propagation effects (convective amplification and Doppler frequency shift), these changes were not observed in equivalent ANOPP-Research predictions.

Above all, this study demonstrates a clear need for improved fan noise and liner attenuation prediction methods, especially given the previously-predicted dominance of these sources on many NASA aircraft concepts. To provide the best possible guidance for future concept development, fan, liner, and PAA prediction methods remain key components to accurate and robust noise assessments. In addition, these methods are critical to evaluating the system-level impacts of noise reduction technologies targeting not just engine/fan noise, but airframe noise as well. Without an accurate accounting of the relative contributions of engine and airframe noise to the system-level noise, predicted component-level effects of noise reduction technologies may not accurately contribute to system-level noise reductions. Future work will endeavor to further process the extensive dataset collected from the various instrumentation systems on this flight test in order to evaluate each fan noise prediction model subcomponent individually, including broadband and tonal noise and inlet- and aft-radiated noise.

Acknowledgments

References

[1] *Strategic Implementation Plan, 2019 Update*, NASA Aeronautics Research Mission Directorate, 2019.

[2] Thomas, R. H., Burley, C. L., and Nickol, C. L., "Assessment of the Noise Reduction Potential of Advanced Subsonic Transport Concepts for NASA's Environmentally Responsible Aviation Project," *54th AIAA Aerospace Sciences Meeting*, San Diego, California, 2016. doi:10.2514/6.2016-0863.

[3] June, J., Clark, I., Thomas, R. H., and Guo, Y., "Far Term Noise Reduction Technology Roadmap for a Large Twin-Aisle Tube-and-Wing Subsonic Transport," *25th AIAA/CEAS Aeroacoustics Conference*, Delft, The Netherlands, 2019. doi:10.2514/6.2019-2428.

[4] June, J. C., Thomas, R. H., and Guo, Y., "System Noise Prediction Uncertainty Quantification for a Hybrid Wing–Body Transport Concept," *AIAA Journal*, Vol. 58, No. 3, 2020, pp. 1157–1170. doi:10.2514/1.j058226.

[5] Thomas, R. H., Guo, Y., Berton, J., and Fernandez, H., "Aircraft Noise Reduction Technology Roadmap Toward Achieving The NASA 2035 Goal," *23rd AIAA/CEAS Aeroacoustics Conference*, Denver, Colorado, 2017. doi:10.2514/6.2017-3193.

[6] Thomas, R. H., and Guo, Y., "Ground Noise Contour Prediction for A NASA Hybrid Wing Body Subsonic Transport Aircraft," *23rd AIAA/CEAS Aeroacoustics Conference*, Denver, Colorado, 2017. doi:10.2514/6.2017-3194.

[7] Bertsch, L., Wolters, F., Heinze, W., Pott-Pollenske, M., and Blinstrub, J., "System Noise Assessment of a Tube-and-Wing Aircraft with Geared Turbofan Engines," *Journal of Aircraft*, Vol. 56, No. 4, 2019, pp. 1577–1596. doi:10.2514/1.c034935.

[8] Guo, Y., Thomas, R. H., Clark, I. A., and June, J. C., "Far-Term Noise Reduction Roadmap for the Midfuselage Nacelle Subsonic Transport," *Journal of Aircraft*, Vol. 56, No. 5, 2019, pp. 1893–1906. doi:10.2514/1.c035307.

[9] Clark, I. A., Thomas, R. H., and Guo, Y., "Aircraft System Noise of the NASA D8 Subsonic Transport Concept," *Journal of Aircraft*, Vol. 58, No. 5, 2021, pp. 1106–1120. doi:10.2514/1.c036259.

[10] Shelts, K. M., Clark, I. A., Thomas, R. H., and Guo, Y., "Aircraft System Noise Assessment of the NASA Single-Aisle Over-the-Wing Nacelle Configuration," *28th AIAA/CEAS Aeroacoustics Conference*, Southampton, United Kingdom, 2022.

[11] *Noise Standards: Aircraft Type and Airworthiness Certification*, Code of Federal Regulations, Title 14, Chapter 1, Part 36, January 2021.

[12] Bradley, M. K., and Droney, C. K., "Subsonic Ultra Green Aircraft Research: Phase I Final Report," NASA/CR-2011-216847, Apr. 2011. URL https://ntrs.nasa.gov/citations/20110011321.

[13] June, J. C., Thomas, R. H., and Guo, Y., "System Noise Technology Roadmaps for a Transonic Truss-Braced Wing and Peer Conventional Configuration," *28th AIAA/CEAS Aeroacoustics Conference*, Southampton, United Kingdom, 2022.

[14] Wong, J., Nesbitt, E., Jones, M. G., and Nark, D. M., "Flight Test Methodology for NASA Advanced Inlet Liner on 737MAX-7 Test Bed (Quiet Technology Demonstrator 3)," *25th AIAA/CEAS Aeroacoustics Conference*, American Institute of Aeronautics and Astronautics, 2019. doi:10.2514/6.2019-2763.

[15] Nark, D. M., and Jones, M. G., "Design of an Advanced Inlet Liner for the Quiet Technology Demonstrator 3," *25th AIAA/CEAS Aeroacoustics Conference*, Delft, The Netherlands, 2019. doi:10.2514/6.2019-2764.

[16] Brusniak, L., Wong, J., Nesbitt, E., Jones, M. G., and Nark, D. M., "Acoustic Phased Array Quantification of Quiet Technology Demonstrator 3 Advanced Inlet Liner Noise Component," *25th AIAA/CEAS Aeroacoustics Conference*, Delft, The Netherlands, 2019. doi:10.2514/6.2019-2765.

[17] Thomas, R. H., Guo, Y., Clark, I. A., and June, J. C., "Propulsion Airframe Aeroacoustics and Aircraft System Noise Flight Research Test: NASA Overview," *28th AIAA/CEAS Aeroacoustics Conference*, Southampton, United Kingdom, 2022.

[18] Czech, M., Thomas, R., Guo, Y., June, J., Clark, I., and Shoemaker, C., "Propulsion Airframe Aeroacoustics and Aircraft System Noise Flight Test on the Boeing 2020 ecoDemonstrator - Program," *28th AIAA/CEAS Aeroacoustics Conference*, Southampton, United Kingdom, 2022.

[19] Krejsa, E. A., and Stone, J. R., "Enhanced Fan Noise Modeling for Turbofan Engines," Tech. Rep. CR-2014-218421, NASA, 2014. URL https://ntrs.nasa.gov/citations/20150000884.

[20] Envia, E., "Fan Noise Source Diagnostic Test - Vane Unsteady Pressure Results," Tech. Rep. TM-2002-211808, NASA, 2002. URL https://ntrs.nasa.gov/citations/20020084621.

[21] Heidmann, M. F., "Interim Prediction Method for Fan and Compressor Source Noise," Tech. Rep. TM X-71763, NASA, 1975. URL https://ntrs.nasa.gov/citations/19750017876.

[22] Kontos, K. B., Kraft, R. E., and Gliebe, P. R., "Improved NASA-ANOPP Noise Prediction Computer Code for Advanced Subsonic Propulsion Systems, Volume 2: Fan Suppression Model Development," Tech. Rep. CR-202309, NASA, 1997. URL https://ntrs.nasa.gov/citations/19970005047.

[23] Guo, Y., and Thomas, R. H., "Assessment of Next Generation Airframe System Noise Prediction Methods with PAA and ASN Flight Test Data," *28th AIAA/CEAS Aeroacoustics Conference*, Southampton, United Kingdom, 2022.

[24] "Standard Values of Atmospheric Absorption as a Function of Temperature and Humidity," *Aerospace Recommended Practice 866, Revision A*, Society of Automotive Engineers, 1975.

[25] Stone, J. R., Krejsa, E. A., Clark, B. J., and Berton, J. J., "Jet Noise Modeling for Suppressed and Unsuppressed Aircraft in Simulated Flight," Tech. rep., NASA TM-2009-215524, 2009. URL https://ntrs.nasa.gov/citations/20090015381.

[26] Thomas, R. H., Czech, M. J., and Doty, M. J., "High Bypass Ratio Jet Noise Reduction and Installation Effects Including Shielding Effectiveness," *51st AIAA Aerospace Sciences Meeting*, Grapevine, Texas, 2013. doi:10.2514/6.2013-541.

[27] Czech, M. J., and Thomas, R. H., "Open Rotor Aeroacoustic Installation Effects for Conventional and Unconventional Airframes," *19th AIAA/CEAS Aeroacoustics Conference*, Berlin, Germany, 2013. doi:10.2514/6.2013-2185.

[28] Hubbard, H., "Aeroacoustics of Flight Vehicles: Theory and Practice, Volume 1: Noise Sources," *NASA Reference Publication 1258*, 1991. URL https://ntrs.nasa.gov/citations/19920001380.